Release of Hydrogen from Nanoconfined Hydrides by Application of Microwaves

Luis Miguel Sanz-Moral[1], Alexander Navarrete[1], Guido Sturm[2], Guido Link[3], Miriam Rueda[1],Georgios Stefanidis[2,4] and Ángel Martín[1]*

[1] High Pressure Processes Group, Department of Chemical Engineering and Environmental Technology, University of Valladolid, Doctor Mergelina s/n,47011 Valladolid, Spain

[2] Process & Energy Department, Mechanical, Maritime & Materials Engineering Faculty, Delft University of Technology, Leeghwaterstraat 39, 2628 CB Delft, The Netherlands

[3] Institute for Pulsed Power and Microwave Technology. Karlsruhe Institute of Technology (KIT). Hermann-von-Helmholtz-Platz-1. 76344 Eggenstein-Leopoldshafen, Germany

[4]Process Engineering for Sustainable Systems Section, KU Leuven Celestijnenlaan 200f – box 2424, 3001 Leuven, The Netherlands

Phone: +34 983184077, e-mail:mamaan@iq.uva.es (Á. Martín)

Release of Hydrogen from Nanoconfined Hydrides by Application of Microwaves

Luis Miguel Sanz-Moral[1], *Alexander Navarrete*[1], *Guido Sturm*[2], *Guido Link*[3], *Georgios Stefanidis*[2,4], *Miriam Rueda*[1], *and Ángel Martín*[1*]

[1] High Pressure Processes Group, Department of Chemical Engineering and Environmental Technology, University of Valladolid, Doctor Mergelina s/n,47011 Valladolid, Spain

[2] Process & Energy Department, Mechanical, Maritime & Materials Engineering Faculty, Delft University of Technology, Leeghwaterstraat 39, 2628 CB Delft, The Netherlands

[3] Institute for Pulsed Power and Microwave Technology. Karlsruhe Institute of Technology (KIT). Hermann-von-Helmholtz-Platz-1. 76344 Eggenstein-Leopoldshafen, Germany

[4]Process Engineering for Sustainable Systems Section, KU Leuven Celestijnenlaan 200f – box 2424, 3001 Leuven, The Netherlands

Phone: +34 983184077, e-mail: mamaan@iq.uva.es (Á. Martín)

Abstract

The release of hydrogen from solid hydrides by thermolysis can be improved by nanoconfinement of the hydride in a suitable micro/mesoporous support, but the slow heat transfer by conduction through the support can be a limitation. In this work, a C/SiO_2 mesoporous material has been synthesized and employed as matrix for nanoconfinement of hydrides. The matrix showed high surface area and pore volume (386 m^2/g and 1.41 cm^3/g), which enabled the confinement of high concentrations of hydride. Furthermore, by modification of the proportion between C and SiO_2, the dielectric properties of the complex could be modified, making it susceptible to microwave heating. As with this heating method the entire sample is heated simultaneously, the heat transfer resistances associated to conduction were eliminated. To demonstrate this possibility, ethane 1,2-diaminoborane (EDAB) was embedded on the C/SiO_2 matrix at concentrations ranging from 11 to 31%wt using a wet impregnation method, and a device appropriate for hydrogen release from this material by application of microwaves was designed with the aid of a numerical simulation.

Hydrogen liberation tests by conventional heating and microwaves were compared, showing that by microwave heating hydrogen release can be initiated and stopped in shorter times.

Keywords: hydrogen storage, hydride, microwave heating, aerogel, supercritical CO_2.

1. Introduction

The increasing share of solar and wind energy in the energetic mix and the COP21 agreement pave the way for a new family of technologies based on renewable energy [1]. Since these renewable energy forms are fluctuating by its nature, it is necessary to develop technologies for storage of energy in periods of excess supply, to use it during the periods of excess demand. Direct use of these energy forms on onboard applications is also not possible, and requires an intermediate form of energy storage.

Storage of this energy in form of hydrogen is one of the most explored methods. The challenge is being addressed using storage systems based on compressed, liquefied and materials-bounded hydrogen [2]. Compared to gas and liquid storage tanks, solid hydrides can store high amounts of hydrogen in small volumes, which usually are liberated by a reversible chemical reaction by thermolysis. However, currently investigated hydrides are limited by slow hydrogen release kinetics or by high thermodynamic stabilities which make it necessary to apply high temperatures to decompose them [3]. Therefore, one of the technological challenges which restrain the development of hydrides for H_2 storage is the heat transfer inside the storage tanks [4]. Great efforts have been made in order to overcome this problem. However, this issue can be circumvented if heating energy is delivered directly to the material, and not by heat transfer through the storage tank. Application of microwaves offers this possibility.

The decomposition of several metal hydrides under microwave irradiation was studied by Nakamori et al. [5]. They concluded that conductive loss and particle size were the two most important parameters controlling H_2 release. Silva Dupim et al. [6] showed that by particle size reduction an

effective heating of the particles was achieved by approximating the size of the particles to the penetration depth of the electromagnetic field in the metallic powder. They obtained this size reduction by applying cold rolling. Another alternative is modifying the dielectric properties of the complex by mixing it with a hydride which actuates as a microwave absorber, as for example $LiBH_4$ [7]. Zhang et al. proposed the use of a honeycomb ceramic monolith coated with 0.54 wt% Ni (corresponding to a thin layer of Ni of 0.2 micron) to hold the hydrides, which allowed the rapid heating of the complex [8].

An alternative to improve the kinetic decomposition of hydrides is using a catalyst [9], but this method adds weight to the complex and sometimes requires the use of expensive metals. Another alternative is the nanoconfinement of the hydride [10, 11]. By confining the hydride inside the porous host, hydride particle size is restrained to the pore size, and particle agglomeration and growth process, which could have an adverse effect on the kinetic decomposition, are avoided. Moreover, some porous hosts, like carbon or silica mesoporous materials, chemically interact with different hydrides and destabilize it, further improving the decomposition kinetics [12]. By combination of these effects, the decomposition temperature and release kinetics can be significantly improved by nanoconfinement. On the negative side, the support materials usually employed, such as mesoporous silica, have very low thermal conductivities that slow down the kinetics of hydrogen release if conventional heating by conduction is applied, and the use of a support material also adds weight to the compound.

However, the mesoporous host can be functionalized to provide additional properties to the material [13]. In particular, it can be functionalized to enhance the absorption of microwave energy, and thus combine the main advantages of the two approaches: nanoconfinement and microwave heating. Indeed, a porous material with a high dielectric lost could confine the hydride and change the global dielectric properties of the complex. A material that fulfills this requirement is carbon, which can be manufactured as mesoporous carbon or as carbon aerogel. Some researchers have already confined hydrides like $NaAlH_4$, $LiBH_4$ [14] or $Mg(BH_4)_2$ into carbon scaffolds [15, 16]. However, these

carbon structures present a limitation which is its low pore volume that restricts the space available for the confinement of hydride inside the support. Due to this limitation, the maximum hydride loadings achieved in carbon matrixes are between 15 and 30% wt., which limits the hydrogen storage capacity below the requirements for practical applications. An alternative could be a hybrid material with leaves more pore space for the confinement of a hydride and provides appropriate global dielectric properties of the complex, making it susceptible to microwave heating. Silica aerogel was already suggested as a very promising material for hydrides confinement due to its remarkable surface properties, and in particular to its high pore volumes that allow confining as much as a 50%wt of hydride [17]. Carbon/silica hybrid aerogels can combine favorable dielectric properties with high pore volumes. Carbon/silica porous materials can easily made by the carbonization of resorcinol–formaldehyde/silica aerogels, as described by Kong et al. [18], keeping favorable textural properties for encapsulation.

In this work, a combined C/SiO_2 porous material susceptible to be heated up by microwaves has been synthesized and impregnated with a hydride. Ethane 1,2-diaminoborane (EDAB) has been chosen as hydride because of its promising properties for H_2 storage: high H_2 content (~10 wt.%) and the absence of undesirable volatile impurities in the released gas [19]. Material characterization and H_2 liberation tests by conventional heating and by application of microwaves have been performed in order to evaluate the possible advantages of application of microwave heating in nanoconfined materials. In addition a numerical simulation of the device under microwaves has been performed to reach better understanding of the process.

2. Materials and methods

2.1 Materials

Resorcinol (R, ≥99% purity from Digma-Aldrich), formaldehyde(F, 36.5-38 % in H_2O from Digma-Aldrich), 3-(aminopropyl)triethoxysilane (APTES, 99% purity from Digma-Aldrich), ethanol(EtOH, 99.5% from Panreac) and technical carbon dioxide (from Carburos Metálicos) were

used for the aerogels synthesis. Technical nitrogen (from Carburos Metálicos) was used for the aerogels pyrolysis. Chlorotrimethylsilane (CTMS, ≥98% from Sigma-Aldrich) and methanol (MeOH, 99.8% from Panreac) was used to functionalize the C/SiO_2 particles. EDAB (96%, from Sigma-Aldrich) and MeOH were used for the wet impregnation of samples.

2.2 Complex synthesis

The resorcinol-formaldehyde aerogels were synthesized following the methodology of Kong et al. [18]. Cylindrical monoliths were made by using R:F:APTES:EtOH, in a molar ratio of 1:2:1:60. After gelation the alcogels were dried by using supercritical CO_2 in order to avoid capillary stresses during solvent removal which could damage de aerogel structure. The drying took place in a closed circuit. The alcogels were placed in a chamber which can be isolated from the rest of the circuit. Then CO_2 was pumped till 10.5 MPa and heated till 40°C. After it the CO_2 was recirculated till the solvent was completely removed. Three loads of fresh CO_2 where needed for a complete drying of the gels. A detailed description of the setup can be found in a previous work [20].

Subsequently the RF/SiO_2 aerogels were pyrolysed in a homemade tubular oven. The samples were heated till 800°C were the T was held for 3 hours. All this process was made under inert atmosphere (~10 $NmLN_2/h$). The pyrolysed monoliths were then milled in a planetary ball mill (PM100 from Retsch) at 100 rpm during 3 h. The resultant powder was immersed in a CTMS MeOH mixture overnight, in order to minimize the hydroxyl and carboxyl content of the matrix surface which could destabilize the impregnated hydride. The rest of the functionalization agent was washed with excess of MeOH.

Finally the powders were loaded with EDAB by wet impregnation, using MeOH as solvent for the hydride (28 mg/mL).

2.3 Material Characterization

The chemical structure of the complex was studied by Fourier Transform Infrared Spectroscopy (FT IR model TENSOR from BRUKER).

The crystallinity of the impregnated EDAB was analyzed by X-ray diffraction (Discover D8-Bruker)

Differential scan calorimetry (DSC) assays were performed with a Mettler-Toledo 822e device. The heating rate was 5°C/min from 30 to 250°C under a N_2 constant flow of 60 mL/min.

The textural properties of the complex were determined by nitrogen isothermal adsorption-desorption. A Surface Area and Porosity Analyzer (ASAP2020from Micrimetrics) was used. The specific surface area was calculated by the BET (Brunauer–Emmett–Teller) method. The specific pore volume was determined by the single point adsorption method. The average pore diameter was calculated with the desorption isotherm of the Barrett-Joynes-Halenda (BJH) method.

The determination of the complex dielectric properties was carried out by means of a cavity perturbation method described by Ramopoulos et al. [21]. Namely, the powdered sample was introduced in a quartz tube (inner diameter 7.8mm) without compaction. 0.49cm^3 of material was tested for samples with ~11%wt EDAB. Then, the sample was introduced at the center of a TE-111 mode cavity with a resonance frequency close to 2.45GHz.

2.4 Numerical simulations. Design of hydrogen liberation cell

The design of the cell used in hydrogen liberation experiments by application of microwaves was supported on a numerical simulation. For this, the process of microwave heating and release of the hydrogen from the material is represented in this work by three basic stages [22, 23]:

1) Generation of the microwaves in the magnetron.

2) Propagation of the electromagnetic waves.

3) Heat generation and transfer in the material.

The model combines all relevant physics. It simulates the electromagnetic interactions in the microwave circuit, including the forward and backward interaction between the applicator section of the circuit and the magnetron microwave source. This was done via microwave network analysis.

The time harmonic stationary microwave field was simulated over the applicator section of the microwave circuit including the load, while the characteristics of the microwave source were represented by an idealized lumped magnetron model. The model characteristics were described in more detail in a previous work [22]. Moreover, the model also included conductive heat transfer. Using the interaction between electromagnetic waves and the material information, the temperature and heat generation were predicted. The medium parameters relevant in the electromagnetics model are the relative permittivity of the materials present in the microwave circuit. The dielectric properties of the composite, measured as described earlier, were introduced in the model. All the simulations were carried out using Comsol Multiphysics® 3.5 [24].

2.5 Hydrogen liberation experiments.

To decompose the hydride and liberate hydrogen, the sample was heated by two different methods:

- By conventional heat transfer, introducing the vessel in a gas chromatography oven (Agilent 7890).
- With a microwave oven (CEM Discover), by placing the vessel vertically, centered and at a high of 3cm from the bottom of the cavity.

Temperature was followed by placing a fiber-optic temperature sensor TS2 (OPTOCOM) inside the internal capillary of the glass vessel. The H_2 flow generated by the thermolysis was measured by a volumetric method by using a fully open mass flow controllers (EL-Flow F-200 from Bronkhorst) with ranges from 0.02 to 1 mL min^{-1}. In these measurements, it was considered that all the released gas was hydrogen. This supposition agrees with available experimental data, which indicates that the gas produced at the operating temperatures considered in this work is nearly pure hydrogen [25]. While the presence of decomposition by-products in the gas cannot be discarded, the presence of

such compounds at minor concentrations would have a negligible influence on hydrogen flow rate calculations, which are the main focus of this work. On the other hand, the presence of these compounds would have a strong impact on the operation as they can damage fuel cells even at low concentrations, and therefore their presence should be evaluated in future works.

3. Results

3.1 Nitrogen isothermal adsorption-desorption isotherms

Table 1 shows the main textural properties of the non-impregnated aerogel and the impregnated ones. Carbon aerogels obtained from the pyrolysis of resorcinol formaldehyde are microporous materials with pore volume under 1 cm^3/g [26]. By contrast, silica aerogels are mesoporous materials with high pore volume (above 2 cm^3/g) [27]. By mixing silica and carbon it is intended to maintain the high the pore volume of silica aerogels, which is important in order to have enough pore space to confine the hydride. Results presented in Table 1 demonstrate that the materials obtained combining silica and carbon have pore volumes above 1 cm^3/g. In the pore diameter distribution, presented in **Figure 1**, two separate regions of micropores and mesopores attributed to the carbon and silica regions are distinguished, with a broad mesoporous size distribution.

As could be expected, by impregnating hydride a significant decrease of the surface area and the pore volume is observed, filling and blocking the smaller pores at this concentration of hydride (~11%). Concerning the isotherms showed on Figure 1, the scaffolds present type IV isotherms, typical of mesoporous materials. In addition, adsorption and desorption branches are almost vertical and nearly parallel over an appreciable range of gas uptake, corresponding to a behavior classified as hysteresis loop H1. This kind of porous material consists of well- aligned, spheres and briquettes [28].

Table 1.Textural properties of the samples.

	BET Surface Area (m^2/g)	t-Plot Micropore Area (m^2/g)	t-Plot External Surface Area	Pore Volume (cm^3/g)	Pore diameter (Ø) (nm)

			(m^2/g)		
C/SiO_2	386	108	277	1.40	21.9
C/SiO_2 + EDAB 11%Wt	216	15	202	1.31	19.4

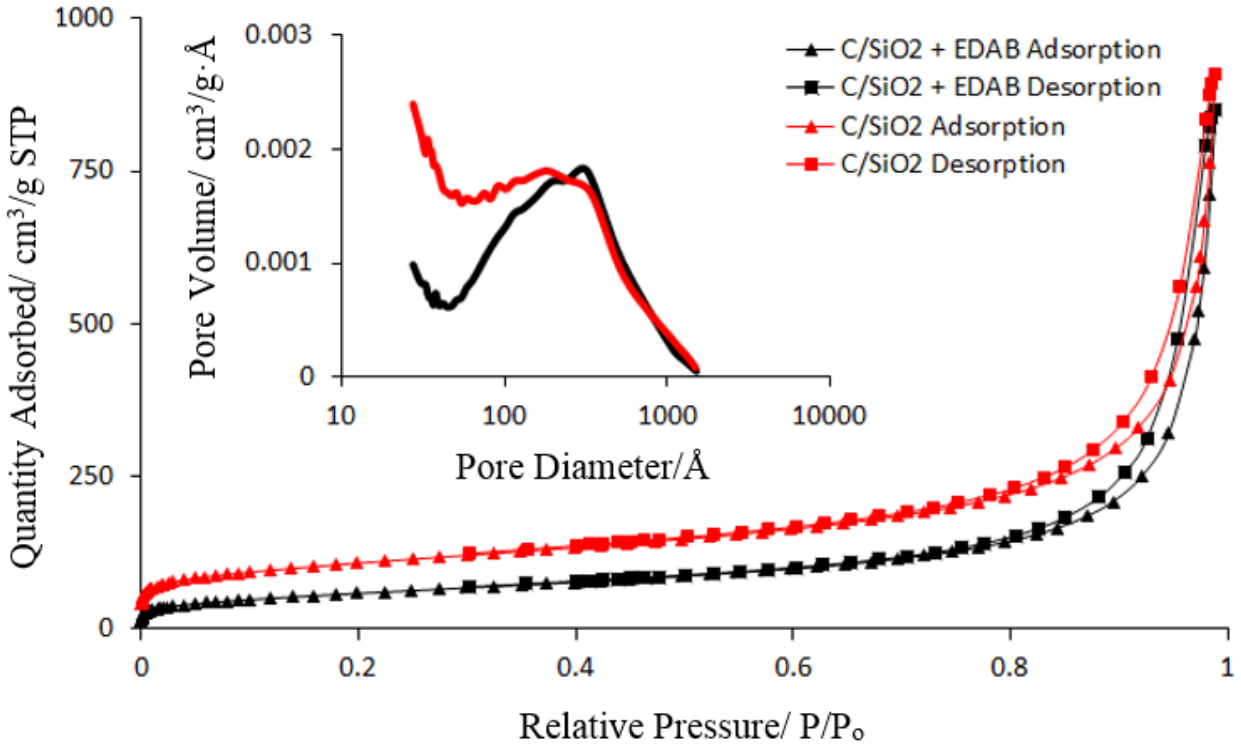

Figure 1. Nitrogen adsorption isotherms and pore size distribution of the raw aerogel and the impregnated one.

3.2 XRD

As shown in **Figure 2**, the XRD pattern exhibited two broad peaks centered at 2θ = 24° and 43°, which corresponded to the 002 and 100 reflection planes of graphite [29]. The diffraction peak around 22° [30], associated with amorphous silica, is overlapped with the diffraction peaks of graphite. Concerning the EDAB peaks, they fit with the raw EDAB pattern reported by Neiner et al. [19]. Therefore no transition phases where observed because of the confinement, and it can be concluded that the hydride is stabilized inside the scaffold without variation of its crystalline structure.

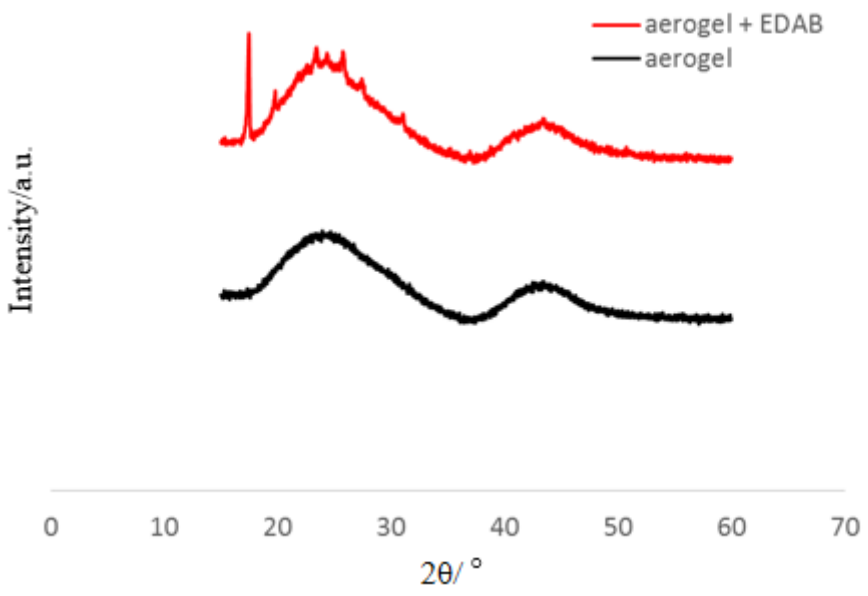

Figure 2. X-ray diffraction patterns of the raw aerogel and the impregnated one.

3.3 DSC

The DSC analyses of the pure EDAB and of the complex impregnated with different EDAB loads are shown in **Figure 3**. Liberation of H_2 on the impregnated samples starts at lower temperatures than in the case of the pure compound. However, the peak of the decomposition takes place at temperatures near 140°C, corresponding to the decomposition temperature of pure EDAB. The samples with the lowest concentration also show a reduction or even disappearance of the right shoulder of the second decomposition step of the EDAB. Both phenomena could be explained by the nanoconfinement effect. This conclusion is supported by the behavior of the complex when the concentration of EDAB is increased: the higher is the concentration, the more similar to the pure compound is the decomposition, indicating that some of the EDAB remains outside of the pores. Some endothermic peaks are observed around 80°C and 100°C, probably due to some residual solvent content or moisture in the sample.

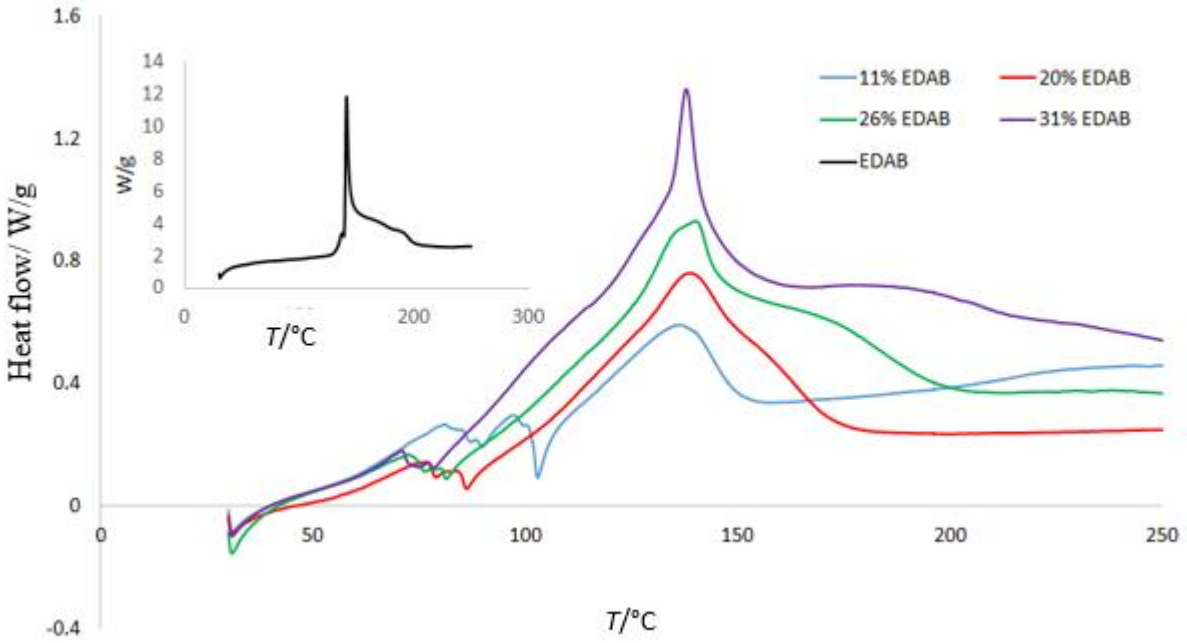

Figure 3. DSC profile of EDAB and the impregnated complex before and after H_2 release.

3.4 Numerical Simulation and vessel design

The results of the dielectric properties of the complex, measured in this work, were ε'=1.24 and ε"=0.26. Taking into account the pore volume of the sample (1.31cm^3/g), which is occupied by air, it is logic that the global dielectric properties are not very different from the air (~1). By contrast the presence of carbon in the matrix has conferred a significant dielectric loss.

Figure 4 shows the simulation results. The 3D electromagnetics model revealed that despite the relatively non-uniform electromagnetic dissipation, the temperature distribution is well homogenized due to small-scale, internal heat conduction. Simulation results demonstrate that the temperature measured in the center of the bed can be considered as representative of the bulk bed temperature, a fact that in this work will be experimentally used to monitor the evolution of temperature in the reactor.

Once the simulations were completed, the glass vessel showed in **Figure 4** was custom-made by Euroglass Instruments, and it was used for the hydrogen liberations. The sample filled the vessel till a high of 2.5 cm, with a density of 0.143g/cm^3.

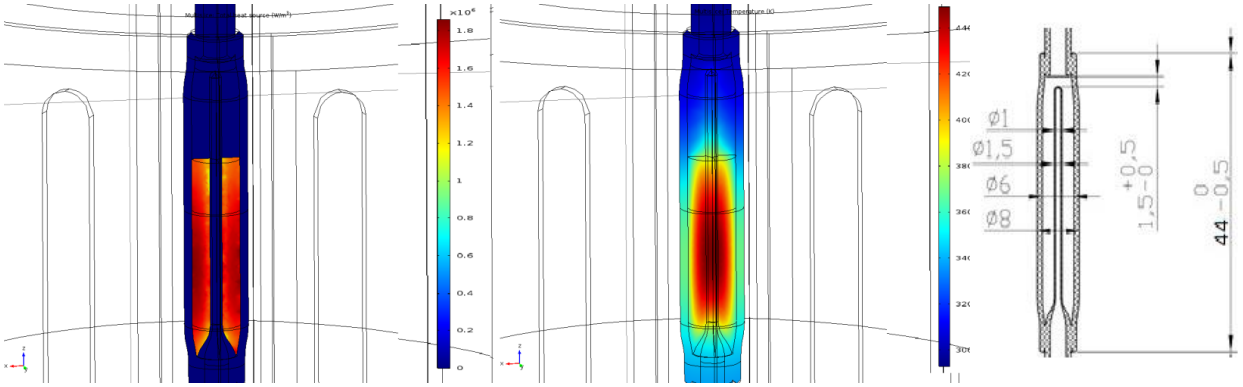

Figure 4. Simulation results. On the left, heat source (W/m^3); on the centre, T (K); on the right, dimensions of the glass vessel

3.5 Hydrogen liberation test

Figure 5 shows the temperature profiles of the sample along the time, obtained by conventional heating in an oven and by microwave heating. The complex used during these tests was the one with ~11% wt content of EDAB. The temperature sensor was placed inside the central capillary of the glass vessel. On one hand, in all the cases, even with the lower powers, the heating rate by application microwaves is higher than the one of the one achieved with the oven. The reason is that in the case of the microwaves, the temperature is increased within all the sample, while the oven heats from outside to the center of the sample, with slow conduction kinetics. On the other hand the temperature profile of the sample heated in the oven is much more stable than the ones heated by microwaves. The temperature gradients along the samples and the expansions of the sample during the heating tests are behind these fluctuations.

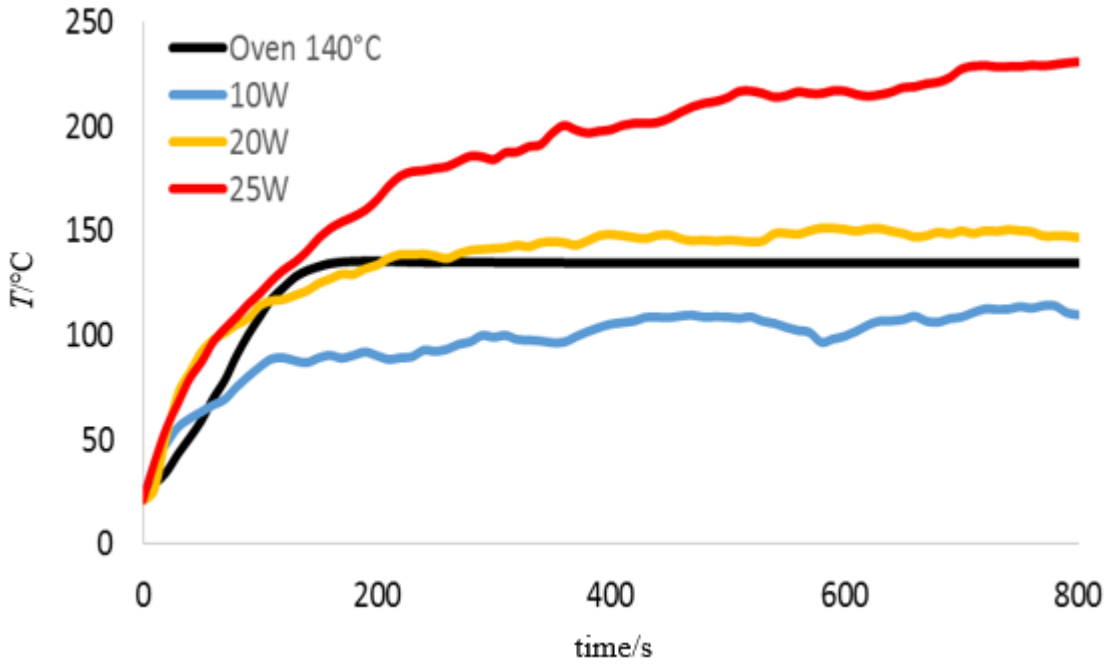

Figure 5. Evolution of temperature during hydrogen liberation tests by conventional heating and by application of microwaves

Figure 6 shows the H_2 flows during the test. Analyzing the thermolysis tests with pure EDAB and nanoconfined EDAB by conventional heating in the oven at 140°C, it can be clearly observed that the nanocofinemnt has an important effect: First, with the nanoconfined sample, hydrogen release starts 85 s after heating is started, while in the case of the pure compound no hydrogen release is observed during the first 200 s. Second, at 140°C the total H_2 released for the complex is much higher than the one of the pure EDAB (91% vs 43%). This phenomena is in good agreement with the DSC profiles, supporting the reduction of the decomposition temperature of the second decomposition step of the EDAB.

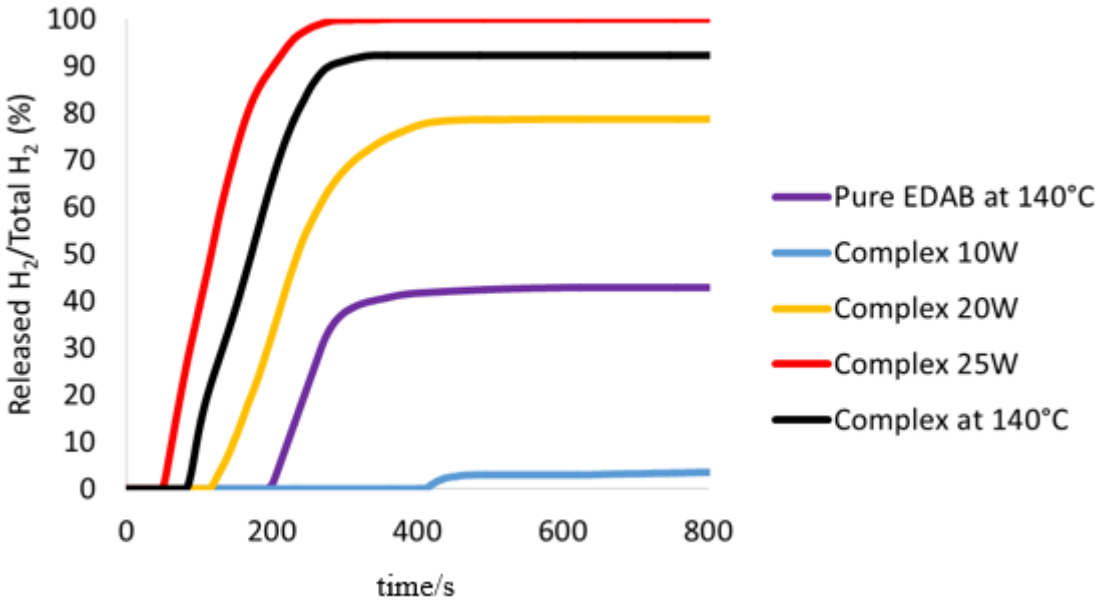

Figure 6. H_2 flow during the liberation tests

In the case of the liberations performed with microwave heating, the one that is reaching the 100% liberation of its H_2 content is the test performed at 25W. As shown in Figure 6, by application of this power, the decomposition temperature of EDAB is surpassed. In the test performed with 20W, the total H_2 liberation was of almost 80%, even though the reached temperature was above 140°C, temperature that in the case of the oven was enough to release above 91% wt of the H_2 content in the sample. The temperature gradients along the sample could explain that some areas have not reached the decomposition temperature, and therefore the H_2 could not be totally released. Finally the test performed at 10W which reaches ~100C°, released just a small H_2 flow. This is in good agreement with the IR spectra of the sample after this test which kept the BH and NH bonds, and supports the stability of this complex at medium temperatures.

Additionally a liberation test was performed by using pulses of 25W along time, simulating the fluctuating energy demand of a real system. Again the liberation did not take place until the decomposition temperature was reached, but hydrogen flow could be easily controlled by stopping the power source and reactivating it. Additionally, as the microwave system just heats up the sample, and not the container, the thermal inertia is reduced in comparison with traditional heating,

and the temperature started to drop as soon as the microwave was stopped. At the end of the test the power was hold till the total amount of hydrogen contained in the sample was exhausted. The results of this test are shown in **Figure 7**.

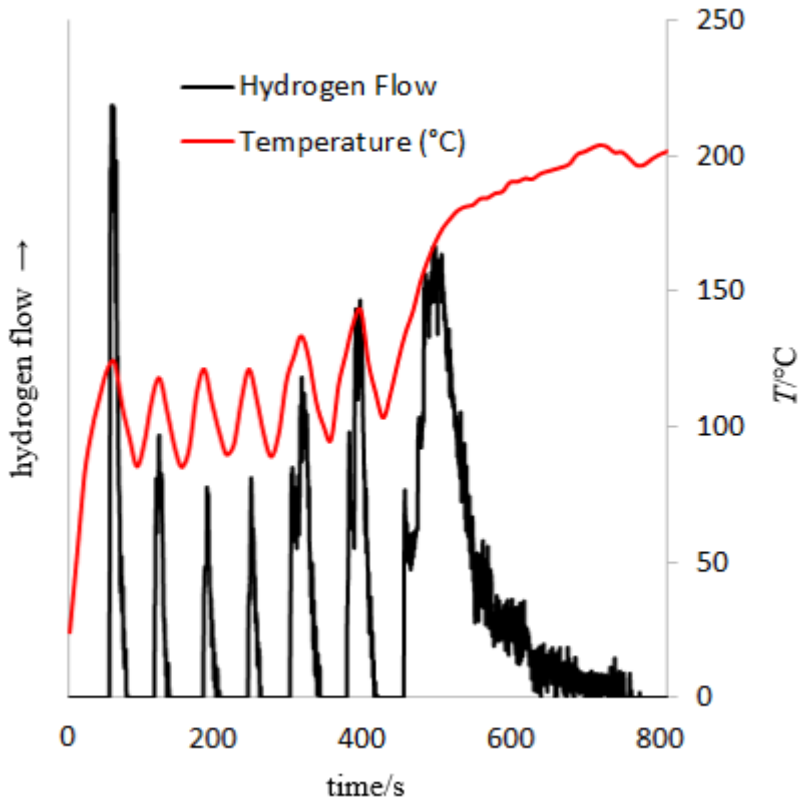

Figure 7. H_2 flow and sample temperature during a liberation test with microwave pulses of 25W

Finally, it must me noted that the reversibility of the hydrogen storage-liberation process is dependent on the hydride compound employed to store hydrogen. As at the moment there is not any procedure available to make the decomposition of EDAB reversible, the proposed compound is not reversible. However, the same methodology proposed in this work could be used with other hydrides that are reversible, such as metallic hydrides.

3.6 IR Spectroscopy

Figure 8 shows the IR spectra of the complex before and after H_2 release tests. The pyrolysed aerogel shows intense silicon–oxygen covalent bond vibrations, appearing mainly in the 1200–1000 cm^{-1}. The very intense and broad band appearing at 1050 cm^{-1} and the shoulder at around 1200

cm^{-1} are respectively assigned to the transversal optical and longitudinal optical modes of the Si-O-Si asymmetric stretching vibrations. On the other hand, the symmetric stretching vibrations of Si-O-Si appear at 800 cm^{-1} [31]. The strong band at 1569 cm^{-1} stems from the aromatic C=C stretching vibrations of the carbons [32]. The broad band centered at around 3100–3600 cm^{-1} corresponds to the overlapping of the O-H stretching bands of surface silanols and carboxylic groups.

Furthermore, the Si-O in-plane stretching vibrations of the silanol Si-OH groups appear at around 960 cm^{-1}. The surface functionalization with CTMS has reduced the intensity of the two OH areas. In addition the band at 1705 cm^{-1} of the untreated carbons related to the carbonyl and the one at 1359cm^{-1} (OCO) [33] have disappeared because of the treatment with CTMS. Instead, CH peak appears at 740 cm^{-1}, 1249 cm^{-1} and 2965 cm^{-1} (CH_3) and the Si-C stretching vibration at 841 cm^{-1}. These two peaks confirms the replacement of some hydroxyl groups by alkyl groups. This functionalization causes a decrease of the oxygen groups on the support surface, avoiding the chemical interactions between EDAB and the support which could destabilize EDAB.

The spectra of the impregnated aerogel shows the typical peaks of EDAB: 702 cm^{-1} of the BN bond; 1039 cm^{-1} of CN bond; 1162 cm^{-1} and 1189 cm^{-1} of BH bond and 1357 cm^{-1}, 1581 cm^{-1},3221 cm^{-1} and 3257 of NH bond. After decomposition, BH and NH peaks disappear, and two new bands at 1326 cm^{-1} and 1362 cm^{-1} grow stronger. These bands are characteristic of B=N stretching, thus evidencing the formation of double bonds between B and N [25]. The only sample which keeps the BH and NH signals after the heating is the one performed at 10W in the microwave. As it was described above, this power was not high enough to reach the decomposition temperature, which justifies the presence of hydrogen bonds in the sample after heating. Furthermore, this result proves the stability of the composite at temperatures below its decomposition temperature.

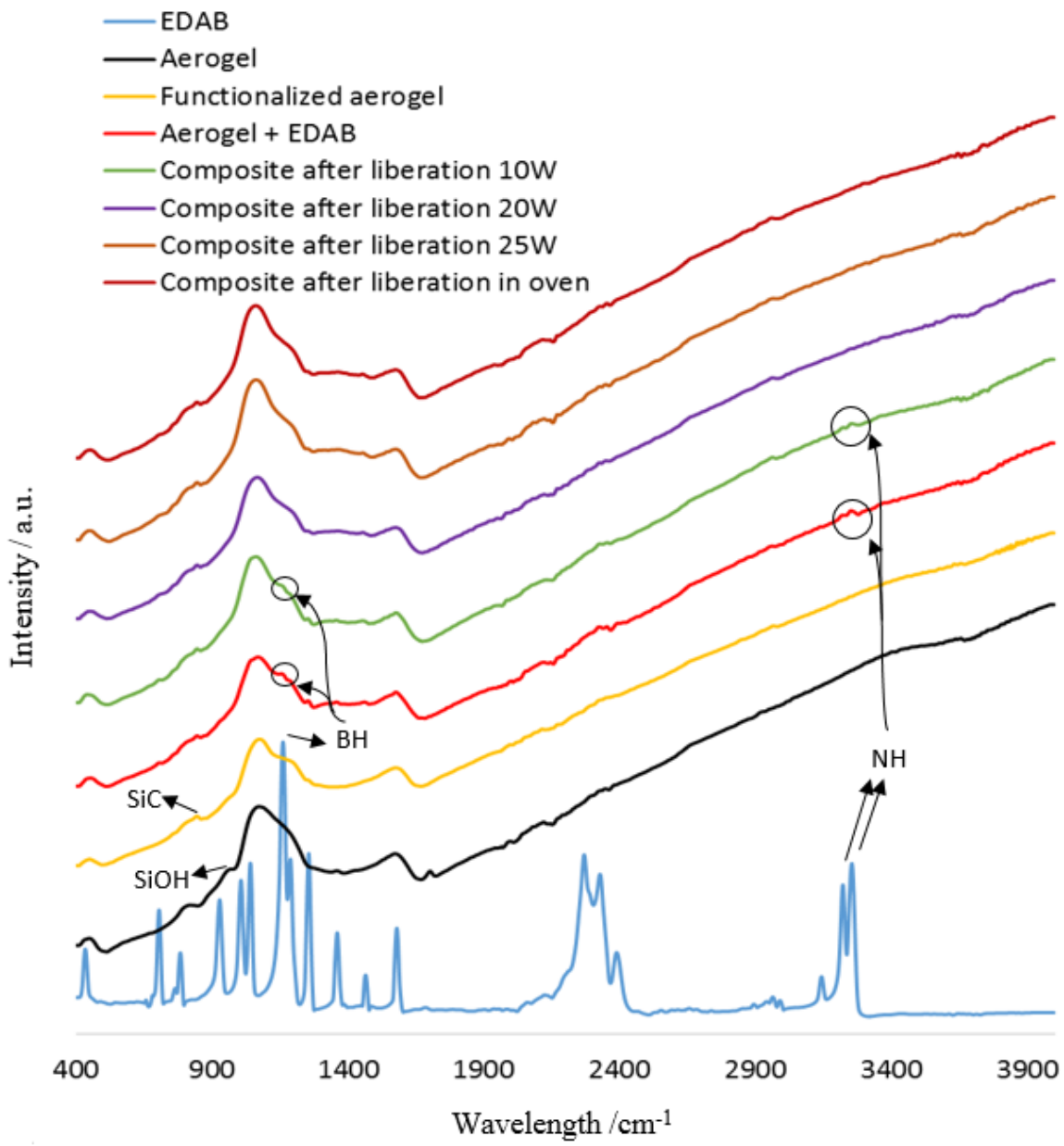

Figure 8. Infrared spectra of EDAB and the impregnated complex before and after the H_2 released.

4. Conclusions

A hybrid C/SiO_2 aerogel has been synthesized and functionalized keeping high pore volume in order to hold EDAB inside its pores. The confinement of the hydride has allowed reducing the response time during the decomposition and has minimized the second decomposition step characteristic of pure EDAB.

The addition of carbon to the matrix has modified the dielectric properties of the matrix and has allowed heating up the system by using microwaves, improving the heating rate. In addition this heating rate could be easily controlled by tuning the power of the electromagnetic field. What is more, the system just heats up the sample, and not the container. Therefore the thermal inertia is reduced in comparison with traditional heating, and the temperature started to drop as soon as the microwave was stopped, allowing controlling the produced hydrogen flow in response to fluctuating demands.

Aknowledgements

This research has been financed by the Spanish Ministry of Economy and Competitiveness through project ENE2014-53459-R. L.M. Sanz-Moral thanks the Spanish Ministry of Economy and Competitiveness for a FPI predoctoral grant.

References

[1] J. Davis. Climate change and the scope for global greenhouse gas reductions. CAB Reviews: Perspectives in Agriculture, Veterinary Science, Nutrition and Natural Resources 11 (2016) 036.

[2] M. Ismail. Effect of LaCl3 addition on the hydrogen storage properties of MgH2. Energy 79 (2015) 177-182.

[3] U. Eberle, G. Arnold, R. von Helmolt. Hydrogen storage in metal-hydrogen systems and their derivatives. J. Power Sources 154 (2006) 456-460.

[4] B. D. MacDonald, A. M. Rowe. Experimental and numerical analysis of dynamic metal hydride hydrogen storage systems. J. Power Sources 174 (2007) 282-293.

[5] Y. Nakamori, S. Orimo, T. Tsutaoka. Dehydring reaction of metal hydrides and alkali borohydrides enhanced by microwave irradiation. Appl Phys Lett 88 (2006) 112104.

[6] I. da Silva Dupim , S. Ferreira Santos, J. Huot. Effect of cold rolling on the hydrogen desorption behavior of binary metal hydride powders under microwave irradiation. Metals 5 (2015) 2021-2033.

[7] H. Y. Leng, J. Wei, Q. Li , K.C. Chou.. Effect of microwave irradiation on the hydrogen desorption properties of MgH2/LiBH4 composite. J Alloy Compd 597 (2014) 136-141.

[8] H. Zhang, H. Geerlings, J. Lin, W.A. Chin. Rapid microwave hydrogen release from MgH2 and other hydrides. Int J Hydrogen Energ 36 (2011) 7580-7586.

[9] S. Milosevic, S. Kurko, L. Pasquini, L. Matovic, R. Vujasin, N. Novakovic, J. Grbovic Novakovic. Fast hydrogen sorption from MgH2-VO2(B) composite materials. J. Power Sources 307 (2016) 481-488

[10] Y Jia, L Cheng , N Pan, J Zou, G.M. Lu, X. Yao. Catalytic De/Hydrogenation in Mg by Co-oped Ni and VO x on active carbon: extremely fast kinetics at low temperatures and high hydrogen capacity Adv. Energy Mater 1 (2011) 387-393.

[11] T. K. Nielsen, F. Besenbacherb, T.R. Jensen. Nanoconfined hydrides for hydrogen storage. Nanoscale 3 (2011) 2086-2098.

[12] M. J. Valero-Pedraza, V. Gascón, M. A. Carreón, F. Leardini, J. R. Ares, Á. Martín, M. Sánchez-Sánchez, M. A. Bañares. Operando Raman-mass specrometry investigation of hydrogen release by thermolyisis of ammonia borane confined in mesoporous materials. Microporous and mesoporous materials 226 (2016) 454-465.

[13] L. M. Sanz-Moral, A. Romero, F. Holz, M. Rueda, A. Navarrete, Á. Martín. Tuned Pd/SiO2 aerogel catalyst prepared by different synthesis techniques. J Taiwan Inst Chem Eng 65 (2016) 515-521.

[14] J. Gao, P. Ngene, M. Herrich, W. Xia, O. Gutfleisch, M. Muhle, K. P. de Jong, P. E. de Jongh. Interface effects in NaAlH4-carbn nanocomposites for hydrogen storage. Int J Hydrogen Energ 39 (2014) 10175-10183.

[15] Y. Yan, Y. S. Au, D. Rentsch, A. Remhof, P. E. de Jongh, A. Züttel. Reversible hydrogen storage in Mg(BH4)2/Carbon nanocomposites. J Mat Chem A 1 (2013) 11177-11183.

[16] Y. S. Au, Y. Yan, K.P. de Jong, A. Remhof, P. E. de Jongh. Pore confined synthesis of magnesium boron hydride nanoparticles. J Phys Chem C 118 (2014) 20832-20839.

[17] M. Rueda, L. M. Sanz-Moral, A. Girella, P. Cofrancesco, C. Milanese, Á. Martin. Reversible hydrogen sorption in the composite made of magnesium borohydride and silica aerogel. Int J Hydrogen Energ 41 (2016) 15245-15253.

[18] Y. Kong, Y. Zhong, X. Shen, S. Cui, M. Yang, K. Teng, J. Zhang. Facile synthesis of resorcinol-formaldehyde/silica composite aerogels and their transformation to monolithic carbon/silica and carbon/silicon carbide composite aerogels. J Non-Cryst Solids 358 (2012) 3150-3155.

[19] D. Neiner, A. Karkamkar, M. Bowden, Y. J. Choi, A. Luedtke, A. Holladay, A. Fisher, N. Szymczak, T. Autrey. Kinetic and thermodynamic investigation of hydrogen release from ethane 1,2-diamineborane. Energ Environ Sci 4(2011) 4187-4193.

[20] L. M. Sanz-Moral, M. Rueda, R. Mato, Á. Martín. View cell investigation of silica aerogels during supercritical drying: analysis of size variation and mass transfer mechanisms. J. Supercrit. Fluids 92 (2014) 24-30

[21] V. Ramopoulos, S. Soldatov, G. Link, T. Kayser, J. Jelonnek. System for in-situ dielectric and calorimetric measurements during microwave curing of resins. GeMiC 2015,16-18, Nürnberg, Germany.

[22] G. S. J. Sturm, M. D. Verweij, T. van Gerven, A. I. Stankiewicz, G. D. Stefanidis. On the effect of resonant microwave fields on temperature distribution in time and space. Int J Heat Mass Tran 55(2012) 3800-3811.

[23] A. Navarrete, R. B. Mato, M. J. Cocero. A predictive approach in modeling and simulation of heat and mass transfer during microwave heating. Chem Eng Sci 68(2012) 192-201.

[24] Comsol Multiphysics 3.5® with RF-module, COMSOL AB Stockholm 2008.

[25] F. Leardini, M. J. Valero-Pedraza, E. Perez-Mayoral, R. Cantelli, M. A. Bañares. Thermolytic decomposition of ethane 1,2-diamineborane investigated by thermoanalytical methods and in situ vibrational spectroscopy. J. Phys. Chem. C 118 (2014) 17221-17230.

[26] T. Horikawa, J. Hayashi, K. Muroyama. Controllability of pore characteristics of resorcinol-formaldehyde carbon aerogel. Carbon 42(2004) 1625-1629.

[27] A. Navarrete, S. Muñoz, L. M. Sanz-Moral, J. J. Brandner, P. Pfeifer, Á. Martín, R. Dittmeyer, M. J. Cocero. Novel windows for “solar commodities”: a device for CO2 reduction using plasmonic catalyst activation. Faraday Discuss. 183(2015) 249-259.

[28] W. Wang, P. Liu, M. Zhang, J. Hu, F. Xing. The pore structure of phosphoaluminate cement. Open J Compos Mater 2 (2012) 104-112.

[29] R. A. Ganeev, P. A. Naik, J. A. Chakera, H. Singhal, N. C. Pramanik, P. A. Abraham, N. R. Panicker, M. Kumar, P. D. Gupta. Carbon aerogel plumes as an efficient medium for higher harmonic generation in the 40-90 nm range. J. Opt. Soc. Am. B 28(2011) 360-364.

[30] W. Xu, A. Du, J. Tang, P. Yan, X. Li, Z. Zhang, J. Shen, B. Zhou. Template confined synthesis of Cu- or Cu2O-doped SiO2 aerogels from Cu(II)-containing composites by in situ alcoholthermal reduction. RSC Adv. 4(2014) 49541-49546.

[31] L. M. Sanz-Moral, M. Rueda, A. Nieto, Z Novak, Z Knez, Á Martín. Gradual hydrophobic Surface functionalization of dry silica aerogels by reaction with silane precursors disolved in supercritical carbon dioxide. J. of Supercritical Fluids 84(2013) 74-79

[32] X. X. Lin, B. Tan, L. Peng, Z. F. Wub, Z. L. Xie. Ionothermal synthesis of microporous and mesoporous carbon aerogels from fructose as electrode materials for supercapacitors. J. Mater. Chem. A 4(2016) 4497-4505.

[33] A. Mattsson, S. Hu, K. Hermansson, L. Österlund. Adsorption of formic acid on rutile TiO2 revisited: an infrared reflection-absorption spectroscopy and density functional theory study. J. Chem. Phys. 140 (2014) 034705.

Figure Captions

Figure 1. Nitrogen adsorption isotherms and pore size distribution of the raw aerogel and the impregnated one.

Figure 2. X-ray diffraction patterns of the raw aerogel and the impregnated one.

Figure 3. DSC profile of EDAB and the impregnated complex before and after H_2 release.

Figure 4. Simulation results. On the left, heat source (W/m3); on the centre, T (K); on the right, dimensions of the glass vessel

Figure 5. Evolution of temperature during hydrogen liberation tests by conventional heating and by application of microwaves

Figure 6. H_2 flow during the liberation tests

Figure 7. H_2 flow and sample temperature during a liberation test with microwave pulses of 25W

Figure 8. Infrared spectra of EDAB and the impregnated complex before and after the H_2 released.